The Branching Angles in Computer-generated Optimized Models of Arterial Trees

WOLFGANG SCHREINER,* MARTIN NEUMANN,‡ FRIEDERIKE NEUMANN,* SUSANNE M. ROEDLER,§ ADELHEID END,* P. BUXBAUM,* MICHAEL R. MÜLLER,* and PAUL SPIECKERMANN‖

From the *Second Department of Surgery, Working Group for Biomedical Computer Simulation; ‡Institute for Experimental Physics, Section for Computational Physics; §Department for Cardiology; ‖Head of the Institute for Medical Physiology, The University of Vienna, A-1090 Wien, Austria

ABSTRACT The structure of a complex arterial tree model is generated on the computer using the newly developed method of "constrained constructive optimization." The model tree is grown step by step, at each stage of development fulfilling invariant boundary conditions for pressures and flows. The development of structure is governed by adopting minimum volume inside the vessels as target function. The resulting model tree is analyzed regarding the relations between branching angles and segment radii. Results show good agreement with morphometric measurements on corrosion casts of human coronary arteries reported in the literature.

INTRODUCTION

Arterial trees feature a high degree of complexity, starting from a feeding artery and then repeatedly bifurcating into smaller branches. Bifurcations may vary between highly asymmetric (when a large vessel gives off a small side branch) and close to symmetric. The endpoint is at any rate to provide adequate supply of blood to each site of tissue within the perfusion area depending on the feeding artery in question.

In the past, the high degree of complexity typical for real vascular trees was usually reduced to several "compartments," each of which represented a certain class of vessels (e.g., arteries, arterioles, capillaries, venules, veins) and was furnished with corresponding parameters for resistance, compliance and (rarely, also for) inertia. In other words, the features of complex structures were reduced and lumped into several parameters ("lumped parameter models"). Within each of the interacting compartments pressure, volume, inflow and outflow were calculated, using coupled differential equations. Thus a detailed description of all hemodynamic quantities was achieved in timesteps typically in the order of milliseconds. However, one severe

Address correspondence to Wolfgang Schreiner, PhD, F.A.C.A., 2nd Department of Surgery, Spitalgasse 23, A-1090 Wien, Austria.

J. GEN. PHYSIOL. © The Rockefeller University Press · 0022-1295/94/06/0975/15 $2.00
Volume 103 June 1994 975–989

drawback was left unsolved: the process of lumping ignores fine structures and hence cannot account for effects arising thereof. Consequently, the desire remained to generate more realistic representations of arterial trees. This was partly done by introducing more and more compartments, each of which still had to reproduce a "lump of vessels."

In the present work, the goal is to generate the structure of an arterial tree from first principles (Thompson, 1952). The model tree's structure, providing all details down to the level of single arterial segments, may then serve as a basis for realistic hemodynamic simulations using differential equations. The "lumping of vessels" for the purpose of hemodynamic simulation is thus rendered unnecessary.

Looking at the corrosion cast of a real arterial tree is fascinating: the complexity, while appearing chaotic on the one hand, still seems to follow some scheme on the other hand, in that the arrangement of arterial segments (i.e., sections between successive bifurcations) comprising a tree is obviously not mere coincidence.

Consequently, the present approach starts with formulating the physiological necessities (i.e., nutrition and oxygenation of tissue) in mathematical terms; these will comprise the first set of boundary conditions to our model. A second set of boundary conditions will be added to guarantee the realistic shrinkeage of vessel radii at bifurcations. In addition to boundary conditions, we finally have to introduce an optimization principle, which will exert a governing influence on the whole development of the tree model.

As a result, we can present a highly detailed model of an arterial tree, which, regarding fineness and complexity, surpasses the models established so far. Finally to demonstrate the realism of the model, the branching angles in the model are compared with experimental measurements on corrosion casts reported in the literature.

PARAMETERS, BOUNDARY CONDITIONS, AND NOTATION

Constraints Derived from the Need for Supply

We assume a certain portion of tissue is to be supplied as homogeneously as possible via a dichotomously branching arterial tree. Each arterial segment (between successive bifurcations) of the tree is represented by a cylindrical tube perfused according to Poiseuille's law (Fung, 1984). Anatomical structures, such as fascia, ligaments or myofibers, which in real organs guide the course of blood vessels, are ignored in the model. We also ignore the fact that the courses of microvessels have to comply with the arrangement of cells in the tissue. Moreover, the piece of tissue is assumed to be flat enough to be represented by a two dimensional area (called "perfusion area"), which we choose to be a circle. Assuming further that, due to similar physiological function, all sub-areas have similar demands in supply, we end up with the following boundary condition for homogeneous supply: the terminal segments of the binary tree model should be distributed as homogeneously as possible over the perfusion area. Each terminal should then deliver the same flow (Q_{term}) of blood against a unique "terminal pressure," p_{term}.

p_{term} is assumed to be the inflow pressure into the microcirculatory network which is not modeled in detail.

Constraints for Radii at Bifurcations

The morphometric analysis of real arterial trees (Zamir and Chee, 1987; Zamir, 1988) has revealed that at bifurcations, the radii of the parent segment together with left and right daughter follow a power law:

$$r_{parent}^{\gamma} = r_{left}^{\gamma} + r_{right}^{\gamma}. \quad (1)$$

Besides the fact that real arterial trees always show some spread rather than exactly fulfilling Eq. 1, all authors agree that the relation is of the above form. However, different values for the exponent γ have been reported in the literature. Measurements on corrosion casts of human coronary arteries (Smaje, Fraser, and Clough, 1980) indicated that $\gamma = 3.0$, which would allow for uniform shear stress all over the tree (Rodbard, 1975). Conversely, it has been argued that minimum reflection of pulse waves (Arts, Kruger, Gerven, Lambregts, and Reneman, 1979) would be achieved with $\gamma = 2.55$.

In the present work, we have limited ourselves to $\gamma = 3.0$, although the method of constrained constructive optimization (CCO) would of course work for arbitrary values of γ (provided that $\gamma > 0$).

Global Parameters

Because the perfusion area represents a piece of tissue, the total perfusion flow (Q_{perf}) and the size of the perfusion area (r_{perf}) must be preset at reasonable and compatible values. For the perfusion bed of a human left anterior descending coronary artery we choose $r_{perf} = 0.05$ m and a reference tissue mass of 100 g. To standardize conditions, we further assume a fully vasodilated state [400 ml/(min × 100 g)] and cardiac arrest. Then, in addition to diastole, the period of systole also becomes available for coronary perfusion, which increases flow by ~25%. Hence, we end up with a reasonable reference value of $Q_{perf} = 500$ ml/min.

Finally, the fineness of the model tree, characterized by the number of terminal segments (N_{term}) must be chosen. Note that the binary branching trees discussed here are allowed to have different numbers of generations along different paths from the root to the leaves. Nevertheless, due to dichotomous branching, the total number of segments is always

$$N_{tot} = 2 \cdot N_{term} - 1, \quad (2)$$

regardless of the particular structure of the tree.

Notations for Specifying a Dichotomously Branching Tree

The dichotomously branching tree (short: binary tree) comprising N_{tot} segments can be specified by (*a*) the geometrical locations, where the coordinates $x(i)$, $y(i)$ refer to the distal (i.e., downstream) end of each segment i, ($1 \leq i \leq N_{tot}$) and (*b*) the connective structure of the tree: for each segment i, we specify the indices of its left and right daughter, D_i^l and D_i^r, respectively. Terminal segments, which do not

bifurcate but rather supply into the microcirculation, have $D_i^l = D_i^r$ = NIHIL. Redundantly and merely for convenience, we also carry a backward pointer to the parent segment (B_i) of each segment i. For the root segment a special index, $i = i_{root}$, is assigned. Although the root segment (by definition) has no parent we may formally assign $B_{i_{root}} = 0$. Then $x(0)$ and $y(0)$ locate the inlet to the tree geometrically.

For example, according to the above notation, the length $l(i)$ of a segment is calculated from

$$l(i) = ((x(i) - x(B_i))^2 + (y(i) - y(B_i))^2)^{1/2}. \tag{3}$$

If segment i has radius $r(i)$, then Eq. 1 (in terms of the above notation) reads

$$r(i)^\gamma = (r(D_i^l))^\gamma + (r(D_i^r))^\gamma \tag{4}$$

and the resistance to laminar flow can be calculated from Poiseuille's law (Fung, 1984):

$$R(i) = \frac{8\eta\, l(i)}{\pi\, r^4(i)} \tag{5}$$

where η is the viscosity of blood in the high shear rate limit. We have verified that our shear rates actually are in this range (i.e., ≥ 100 s^{-1}; Milnor, 1989). Also, the maximum Reynolds number observed in the segments of our model was always well below 2300, the upper limit for laminar flow, so that in principle Poiseuille's law should be applicable.

Furthermore, it is convenient to define bifurcation ratios to characterize the relative shrinkeage of radii when branching into the left and right daughter of a parent segment:

$$\left.\begin{aligned} \beta^l(i) &= r(D_i^l)/r(i) \\ \beta^r(i) &= r(D_i^r)/r(i) \end{aligned}\right\} \tag{6}$$

THE CONCEPT OF CONSTRAINED CONSTRUCTIVE OPTIMIZATION

The Possibility of Flow-scaling

Suppose a binary tree has been (partly) defined by specifying all coordinates and (forward) pointers: $\{x(i), y(i), D_i^l, D_i^r; i = 1, \ldots N_{tot}\}$. We will show that it is always possible to scale the segments' radii such that (*a*) all terminal segments yield equal flows at equal pressures; (*b*) the bifurcation law (Eq. 4) is fulfilled at each bifurcation; and (*c*) the resistance of the tree as a whole can be set to permit a (deliberately chosen) total perfusion flow Q_{perf} across the overall pressure gradient $\Delta p = p_{perf} - p_{term}$.

The proof can be given as follows. First consider a segment i branching into two terminal segments. Because both terminal segments originate from the same bifurcation, they experience equal inlet pressures. Because both drain into the microcirculation, they also experience equal outlet pressures (p_{term}) and hence equal pressure drops. Given their lengths, the ratio of radii $r(D_i^l)/r(D_i^r)$ can always be chosen to yield

equal resistances

$$(r(D_i^l)/r(D_i^r))^4 = 1(D_i^r)/1(D_i^l). \tag{7}$$

This will guarantee that equal flows leave these two terminals, as required by the perfusion constraint formulated above. Inserting $r(D_i^l)/r(D_i^r)$ into the bifurcation rule (Eq. 4) yields bifurcation ratios via Eq. 6. If the latter are held constant, equal flows will be carried through both terminals even for arbitrary radius of the feeding segment i.

Next we realize that segment i and its two daughters may be regarded as a subtree and realize the following: for any positive gradient between the inlet pressure into segment i and p_{term}, and while keeping bifurcation ratios constant, $r(i)$ can always be chosen such that the subtree carries a flow of exactly $2 \cdot Q_{term}$ (as it should be).

Without rigid proof we conclude the following to hold for arbitrary subtrees: bifurcation ratios within the subtree are set to achieve proper (relative) splitting of flow down to the terminal level, while the radius of the inlet segment controls total flow into a subtree without having any effect on the splitting of flow.

Finally, we consider a bifurcation into two subtrees, each of which we assume to have its bifurcation ratios set appropriately. Then we can always balance the radii of the inlet segments such that the flows into the subtrees are in the same proportion as the respective number of terminal sites supplied. As a result, terminal flows are not only equal within subtrees but also between subtrees. Because any binary tree can be assembled from subtrees, it is possible to implement the homogeneous perfusion constraint all over the entire tree, as required. In other words: flow balancing and scaling is possible regardless of the particular structure of the tree.

Geometric Optimization

Given a flow-scaled tree which fulfills the bifurcation rule. Then we may adopt a target function T characterizing the degree of optimality of the tree in question. The selection of T is arbitrary in principle, and various candidates have been proposed (Lefevre, 1983). Presently, we restrict the analysis to a very simple form of T, namely the minimum total intravasal volume of the tree:

$$T = V = \pi \cdot \sum_{i=1}^{N_{tot}} 1(i) \cdot r^2(i) \Rightarrow \text{minimum}. \tag{8}$$

Note that given locations $(x(i), y(i), i = 1, \ldots N_{tot})$ automatically define segment lengths $1(i)$. The implementation of proper flow splitting (as described above) induces bifurcation ratios $(\beta^l(i), \beta^r(i))$, and the required total flow (Q_{perf}) is achieved by the appropriate setting of $r(i_{root})$.

Suppose we select one bifurcation segment, say segment j, and displace it (without changing the tree's topology). As a consequence, (most likely) all three segments forming the bifurcation will change in lengths and resistances, and make the tree violate the boundary conditions. These can be reestablished, however, by reassessing all bifurcation ratios affected and $r(i_{root})$. However, the new tree will in general have a volume (i.e., target function) different from what it was before the move of the bifurcation.

Hence, intravasal volume may be interpreted as a continuous function of all coordinates $V = V(x(i), y(i), i = 1 \ldots N_{tot})$ if topology (i.e., the connective structure) of the tree remains unchanged. Thus, bifurcations can be moved along the gradients towards minimum target function by an iterative method, while all boundary conditions (constraints) are fulfilled at each step of the iteration (constrained optimization). Of note is the fact that this kind of optimization can only lead to a local minimum of T within the topology chosen.

Structural Optimization

Trees with equal numbers of segments, but different in topologies, will, upon optimization of all bifurcations, in general lead to different minimum values of the target function. Hence, minimum T is a function of topology, the latter being represented by the set of pointers:

$$T_{min} = T_{min}\,(D_i^1, D_i^r, i = 1, \ldots N_{tot}). \tag{9}$$

Note that:

$$\text{all possible sets of pointers} = \{(D_i^1, D_i^r, i = 1, \ldots N_{tot})_k\} \tag{10}$$

form a finite and discrete but enormously large set, even for moderate values of N_{tot}. We have to select that topology which is able to yield the global minimum of the target function. It would by far exceed the computational resources presently at hand to generate all possible topologies one after the other, optimize each and finally select the global optimum. It is a key point of the present work to introduce the method of constrained constructive optimization (CCO) instead.

The key idea is as follows. We start with a degenerate tree comprising one segment only. Its distal end is selected randomly within the perfusion area. The radius is adjusted so as to convey the flow Q_{term}. Then, the location for the distal end of a second terminal segment is chosen, and its proximal end connected to the midpoint of the first segment, thereby generating the first bifurcating segment (now three segments altogether). While keeping the distal ends of the two terminal segments as well as the inlet to the root at their positions, the bifurcation is moved in steps (within the perfusion area) along descending gradient into a position yielding the minimum total volume for the three-segmental tree. Note that after each move, bifurcation ratios and $r(i_{root})$ have to be rescaled in order to reimplement the fulfillment of boundary conditions.

Next, the location for the distal end of a third terminal segment is chosen from pseudo random numbers. It is checked that this location is not too close to any of the preexisting segments. This "vicinity check" is performed in a nested loop: for the trial location we calculate the minimum distance to the centerlines of all existing segments. If this minimum distance exceeds a threshold, the new terminal location is accepted; if not, tossing is repeated up to 10 times. In case no acceptable position has been found, the threshold is decreased by a factor 0.9 and another loop of 10 times tossing is resumed. Before adding a new terminal, the threshold is initially set proportional to the space available per terminal site $(r_{perf}^2/k_{term})^{1/2}$, where k_{term} is the current number of terminal segments, and decreases as more and more segments are

added. Note that as a consequence, the distribution of terminals is much more uniform than if they were drawn from a random distribution.

After being generated, the new terminal is arbitrarily connected to the first segment. The new bifurcation is optimized and the (local !) minimum of T recorded. Note that T is considered valid only if the new segment in its optimized geometrical position does not intersect with any of the preexisting segments (except for its sister and parent). In any case, the connection is dissolved again and the process of testwise connecting the new terminal is repeated for all preexisting segments in the vicinity of the new terminal site. Actually, this testwise connection is only performed for the N_{close} segments nearest to the new terminal site ($N_{close} = 100$). Thus in early stages of growth (as long as $N_{tot} \leq N_{close}$), the connection search extends over the whole tree, but it is restricted to a diminishing portion of the tree later on. Finally, that connection site which allows the utmost minimization of T within one lap of connection search is adopted to become permanent.

It is interesting to note that an optimally connected terminal never intersects with any of the preexisting segments (except for its parent and sister), even though the algorithm does not explicitely preclude intersections. During the connection search, suboptimum connection sites are examined and intersections do occur. However, topologies with intersections were never seen to yield the minimum value of the target function and hence are not allowed to become permanent. This is reasonable, because the intersected (preexisting) segment itself usually provides a more suitable connection site (which is closer and offers a lower target function in terms of volume within segments) than the (more remote) connection site currently tested. This parallels our intuition that the nearest site of intersection should rather be chosen for connection.

Repetition of the whole process described above grows the model tree, step by step, and is able to create trees comprising several thousand segments. Note that the model at each stage of development meets the very same physiologic conditions we require the complete tree to fulfill.

RESULTS

A Typical Realization

Constrained Constructive Optimization has been implemented on an IBM 3090 mainframe computer at the Institute for Medical Informatics at the University of Vienna, Austria. Choosing minimum intravasal volume to be the target function, a tree with 4000 terminal segments (and hence 7999 segments in total) can be grown in $\sim$50 h of computation time. Fig. 1 displays a typical result, the diameters of the cylindrical segments appearing as widths of the branches in the display.

Distribution of Branching Angles

Out of the many quantities available from the model we focus on the distribution of branching angles in relation to the ratio of radii at bifurcations. These relations have also been investigated experimentally in the human coronary arterial tree (Zamir and Chee, 1986), and hence model results may be directly compared with reality. Please note that neither anatomical information nor any kind of parameters relating to

branching angles have a priori been plugged into the model. We rather let branching angles develop from the model itself. If they are still reproduced realistically, this may count as a convincing indicator for model validity. ZAMIR (Zamir and Chee, 1986) reports on measurements in two coronary trees with 500 and 350 bifurcations respectively, and hence we also generated a tree with 500 terminal and 499 bifurcating segments for comparison. In its major branches this tree is similar to the one with 4,000 terminal segments shown in Fig. 1, but the very small segments are omitted. At each bifurcation site of the model tree the two branching angles θ_1 and θ_2 were calculated (cf Fig. 2) and plotted over the ratio of daughter radii r_2/r_1. In accordance with the experimental work of ZAMIR, subscript 1 always refers to the segment with the larger, and subscript 2 to the segment with the smaller radius ($r_2 \leq r_1$). Fig. 3 shows the distribution of θ_1 (i.e., the branching angle of the thicker

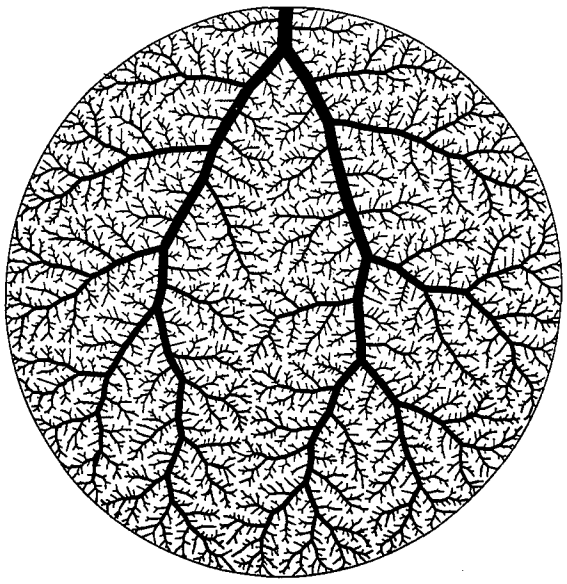

FIGURE 1. Model for an arterial tree with 4000 terminal segments. Optimization was performed for minimum volume inside the vessels. Note that no anatomical information whatsoever has been plugged into the model and structure emerges entirely from optimization.

daughter), each data point representing one particular bifurcation. Fig. 3 (*left*) shows the model results, whereas the right panel (labeled *Corrosion Cast*) shows the experimental results from (Zamir and Chee, 1986). In accordance with the experimental measurements the model yields a rising tendency of θ_1 with increasing r_2/r_1 and values of θ_1 larger than 40° occur but are rare. Also the spread of θ_1 is comparable to the experimental findings.

Interestingly, the visual inspection of Fig. 3 (*left, Model*) suggests to discriminate two subgroups of bifurcations, each showing a different dependence on r_2/r_1. In the first group, data points (*open squares*) seem to form a cluster in the shape of a cone, with its axis representing a rising tendency for increasing r_2/r_1. Within the second cluster (*solid squares*) there is less spread and data points seem to gather around an arc connecting ($\theta_1 = 0°$, $r_2/r_1 \cong 0.6$) and ($\theta_1 \cong 35°$, $r_2/r_1 = 1$), cf Fig. 3.

It took some time to find out that in fact a very simple criterion excellently discriminates between the two groups: Let

$$\mathrm{NDIST}_i = \left\{\begin{matrix}\text{number of terminal segments}\\ \text{distal (=downstream)}\\ \text{of segment } i\end{matrix}\right\}. \tag{11}$$

Then we may form one group with $\mathrm{NDIST}_i = 2$, representing those segments branching into nothing but *two* terminals. These are shown as solid squares in Fig. 3 and obviously constitute the ensemble we are looking for. The second group (*open squares*) comprises all other cases $\mathrm{NDIST}_i > 2$. Further splitting within group 2 failed to offer any additional power of discrimination.

In addition to the branching angles obtained from our model, Fig. 3 also shows a solid curve representing a theoretical prediction for θ_1 given by ZAMIR (Zamir, 1978). He derived that, for minimum lumen volume, the following relation should be valid:

$$\cos\theta_1 = \frac{(1+\alpha^{3/2})^{4/3} + 1 - \alpha^2}{2(1+\alpha^{3/2})^{2/3}}, \qquad \text{with} \qquad \alpha = (r_2/r_1)^2 \tag{12}$$

If both daughters have equal radii, $\theta_1(\alpha = 1) = 37.5°$ is predicted.

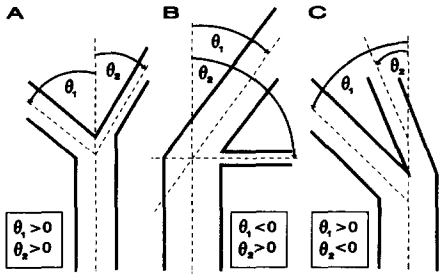

FIGURE 2. Definition of branching angles. Schematic (nonquantitative) display of the three possibilities for positive and negative branching angles. (*A*) Usual configuration $\theta_1 > 0$, $\theta_2 > 0$. (*B*) Major branch with negative angle $\theta_1 < 0$, $\theta_2 > 0$. (*C*) Minor branch with negative angle $\theta_1 > 0$, $\theta_2 < 0$.

Fig. 4 compares the values of θ_2 obtained from the model with those measured by ZAMIR. He also gave the theoretical prediction

$$\cos\theta_2 = \frac{(1+\alpha^{3/2})^{4/3} - 1 + \alpha^2}{2\alpha(1+\alpha^{3/2})^{2/3}} \tag{13}$$

In the model, the distribution of θ_2 also suggested two groups to be discriminated in the same way as for θ_1. Again, the angular distribution obtained from the model for $\mathrm{NDIST} > 2$ closely resembles measured data (Zamir and Chee, 1986) in showing a declining trend from rectangular (for highly asymmetric bifurcations) to 30 to 40° near $r_2/r_1 = 1$. Of note, because $\theta_1 = \theta_2$ for a symmetrical bifurcation, Eqs. 12 and 13 (must) yield equal predictions for $\alpha = 1$: $\theta_1(\alpha = 1) = \theta_2(\alpha = 1) = 37.5°$.

Considering the total angle $\theta_1 + \theta_2$ between both daughters, again we find a good agreement with the study of corrosion casts (Zamir and Chee, 1986), see Fig. 5. Starting at 90°, the trend is slightly falling towards symmetric bifurcations, approaching the theoretical limit of $2 \cdot 37.5° = 73°$. Similar to the individual distributions, the

total angle $\theta_1 + \theta_2$ also forms separate clusters for bifurcations with $NDIST_i = 2$ and $NDIST_i > 2$.

DISCUSSION

Comparison between Model Results and Branching Angles in Real Coronary Artery Trees

When comparing the branching angles in the model with measurements on corrosion casts, we have to bear in mind that no anatomical information whatsoever has been plugged into the model, and all structural features have solely emerged from the governing influence of the optimization principle under the constraint of appropriate

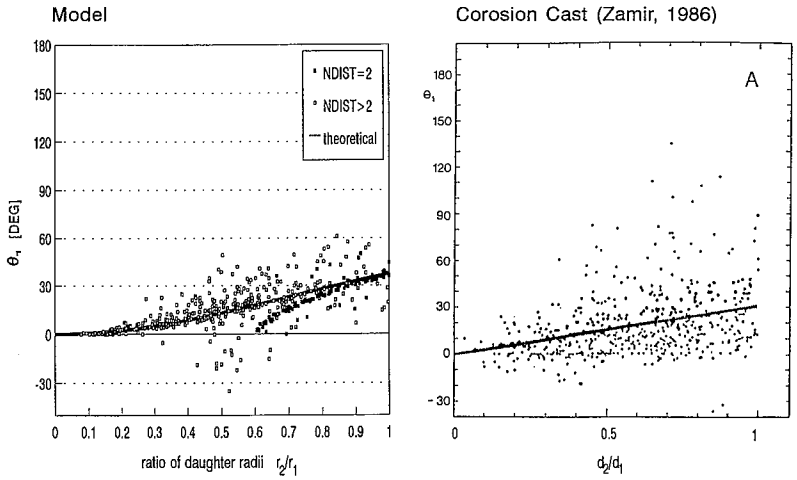

FIGURE 3. Branching angles of the major daughters. According to the definitions shown in Fig. 2 the branching angle of the daughter with the larger radius is shown on the vertical axis. (*Horizontal axis*) Ratio of daughter radii, r_2/r_1. Data from the model (*Model*) are reported in exactly the same form as the experimental data in the literature *Corrosion Cast/(ZAMIR 1986)* (reproduced with kind permission by the National Research Council, Canada). (■) Segments with NDIST = 2; (□) NDIST > 2. (*Solid line*) Theoretical prediction of optimum branching angles for constant shear stress and minimum lumen volume.

boundary conditions. Hence, any accordance with a real arterial tree can be seen as a positive test for the parameters chosen and the method of constrained constructive optimization itself.

In general, the distributions of branching angles obtained from the model resemble those found experimentally (Zamir and Chee, 1986). In particular the following similarities may be discussed.

Regarding the branching angle of the larger daughter (Fig. 3) we realize that at highly asymmetric bifurcations, i.e., when a major artery gives off a tiny branch ($r_2/r_1 \ll 1$), the major artery proceeds almost in its previous direction (small value of θ_1). Conversely, for bifurcations close to symmetric ($r_2/r_1 \cong 1$), the majority of angles

is found between 30 and 40°, which is similar to the experimental results and in agreement with the theoretical prediction (37.5°).

The branching angles of the smaller daughters (Fig. 4) are close to rectangular for highly asymmetric bifurcations and show a declining tendency as bifurcations become more and more symmetric. It is remarkable, however, that only a small percentage of angles θ_2 are larger than theoretically predicted, whereas the distribution of θ_1 appears fairly balanced around the theoretical estimate.

In accordance with the experimental results, the model yields (a small portion of) negative branching angles down to $\sim -30°$. First we realize that a priori only one (either θ_1 or θ_2) can be negative, because otherwise, we would simply have to swap (i.e., exchange) indices 1 and 2, cf Fig. 2 *b*. Second, one negative angle indicates that both daughter segments branch to the same side, relative to the parents' axis. If θ_1 is negative, it follows that the smaller branch aberrates more from the parent's axis

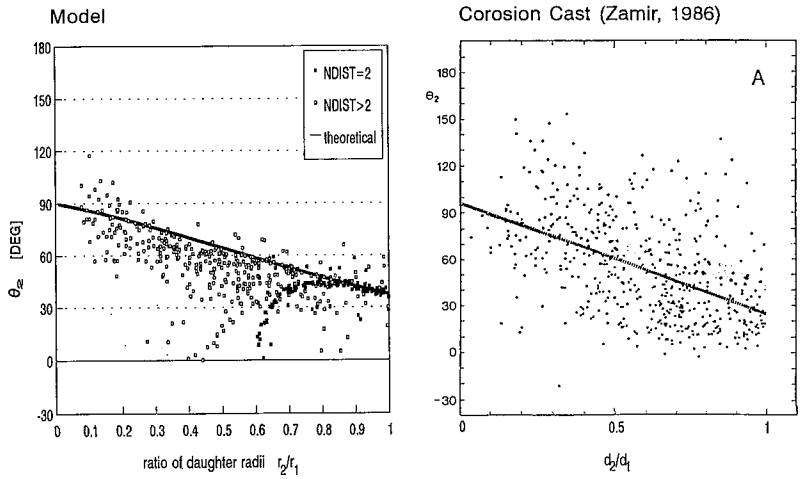

FIGURE 4. Branching angles of the minor daughters. Notation similar to Fig. 3. (Right panel reproduced with permission by the National Research Council, Canada.)

than does the larger one: $\theta_2 > |\theta_1|$, cf Fig. 2 *b*. This case is frequently seen in both the corrosion casts and the model. Conversely, $\theta_2 < 0$ implies that the smaller branch deviates less from the parent's direction than does the larger one: $|\theta_2| < \theta_1$, cf Fig. 2 *c*. Again, in agreement with experimental results, only very few such cases occur in the model.

An interesting question is "why do we find negative branching angles at all ?" Obviously they are exceptional and seem to violate what we would expect to result from an optimization. But still they occur.

Regarding real coronary arteries we can nothing but speculate what the reason might be. (*a*) Anatomic substructures (e.g., the direction of the myofibers) may enforce angular deviations. (*b*) We cannot expect real arteries to obey mathematical laws exactly. Deviations may be nothing but the normal and ordinary biological spread encountered throughout the life sciences.

All in all, negative angles in real trees are not really a puzzle. In computer generated trees however, which we claim to be optimized, the need for an explanation becomes urgent. In fact, it can be given as follows.

It is true that optimizing the position of a bifurcation for minimum intravasal volume can never yield a negative branching angle for one of its daughters. However, a branching angle also changes if one daughter should change direction. The latter occurs whenever a new terminal is connected to that daughter and the newly generated bifurcation is then optimized. In the majority of cases, angles change but remain positive, in some cases they switch to negative, however. Because either daughter can become the parent of a new terminal, negative angles may occur for the smaller as well as for the larger daughter.

The reason for negative branching angles to occur in the model is the fact that bifurcations proximal to a site of growth of the tree are not reoptimized. The location

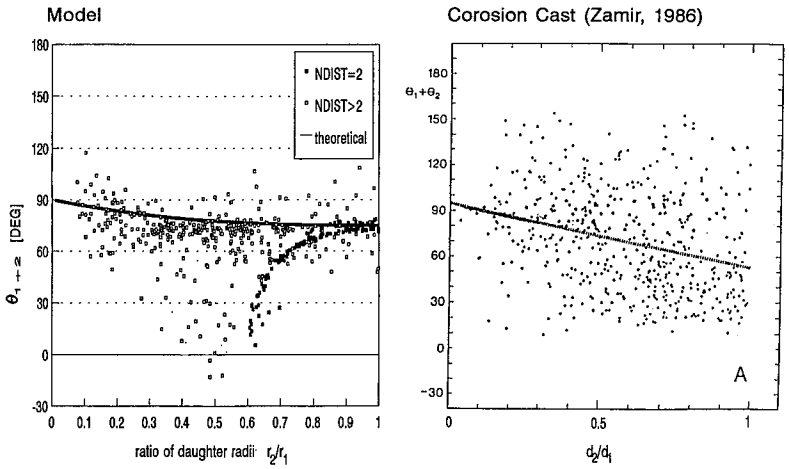

FIGURE 5. Angles between both daughters. The sum of angles, $\theta_1 + \theta_2$, is displayed in symbols similar to Fig. 3. (Right panel reproduced with permission by the National Research Council, Canada.)

of such a proximal bifurcation, which was optimized in a preceeding step of growth, is no longer optimum within the final tree. The model kind of inherits structures from previous stages of development, which is a remarkable analogy to phyllogenetic development.

The computer model could be generated even to overcome this natural deficiency. In addition to balancing the bifurcation ratios, we could also reoptimize the location of each bifurcation proximal to a site where a new terminal was attached. This would in fact mean that even established vessel segments may slightly change their locations as a result of adding new branches. This process would mimic some kind of secondary adaption process triggered by growth in distal subtrees. At present, we can only state that it would be interesting to investigate if this finds a parallel in reality.

Considerations Regarding Dimensionality

A major assumption of the present model is that the tissue to be perfused is two-dimensional. In fact, the geometry of a small tree of arteries (16 terminals) in the mesentery of a dog (considered representative for a two-dimensional t issue) has been investigated experimentally (Kamiya and Tatsuo, 1972). A model of tubes with the same given topology was established and the geometric locations of bifurcations were optimized according to minimum intravasal volume. Because the result was seen to reproduce the geometry found in the mesentery, we may consider minimum volume to be a reasonable optimization target.

Another question is if and how the model, which is currently two-dimensional, could be generalized to three dimensions. We have to discriminate three different cases.

(*a*) The two-dimensional surface is not flat any more but curved in space, e.g., like the retina in the eye. Then we may assume that the centerlines of all segments lie, e.g., on the surface of a sphere and are great circles. In this case, a different representation of geometrical coordinates and distances suffices to generalize the model.

(*b*) We consider a real three dimensional, volume-filling part of tissue which is convex, homogeneous and isotropic. A possible candidate may be the liver. In this case the extension to three dimensions requires us to use (x,y,z) instead of (x,y) as geometrical coordinates, which is conceptually straight forward.

(*c*) A conceptual addition becomes necessary, however, when we consider organs like the ventricle of the heart: coronary arteries must not cross through the ventricular chambers but run entirely within the ventricular wall; and phasic intramyocardial pressure increases from epi- to endocardium and may cause endocardial segments to collapse during systole. Consequently, the main conveying vessels run at the epicardial surface. To incorporate these features within the framework of the present model, additional assumptions would become inevitable, and we rather restrict the present work to display the concepts of CCO together with key results.

Conclusions and Synopsis for Previous Models and CCO

In general, the modeling of arterial trees may follow one of four different lines.

Lumped parameter models. They condense features of complex structures into representatives (i.e., compartments).

Detailed anatomical modeling. Morphometric parameters, such as lengths of segments, radii and the real branching geometry are implemented in a model to represent a certain vessel and its major branches in detail and specifically (Rooz, Weisher, and Nerem, 1985). Typically, these models consider a few dozen segments.

Deterministic and stochastic fractal modeling. In the deterministic approach, known features of real arterial trees, such as the average shrinkeage of segment lengths and radii, are used as a basis. Starting from the root, segments are generated for several bifurcation orders, with all parameters changing in a fully determinstc way from one bifurcation order to the next (West and Goldberger, 1987; Pelosi, Saviozzi, Trivella, and L'Abbate, 1987). (The law according to which parameters are to be changed is called the generator). The result is a structure which is self-similar regarding the

parameters considered: subareas on a smaller scale repeat the properties already seen on a larger scale. These models are evaluated to check if an appropriately designed self-similar structure is able to reproduce the key features of its real counterpart in a statistical sense, and if so, can we simultaneously expect the hemodynamic properties (volumes, resistances, compliances) to match?

However, even if all quantities match, there is no guarantee that it will be possible to arrange such a structure in space. Consequently, the possibility of arrangement in space is considered a further criterion in the selection of generators.

In the stochastic approach (Dawant, Levin, and Popel, 1985; Levin, Dawant, and Popel, 1986), spread is added to the generator in that the transition laws from one order to the next become stochastic, e.g., with given mean and standard error. These models overcome the rigidity of deterministic fractal models and thus can (in principle) get closer to reality. The question of arrangeability in space, however, is even more complicated to answer than for deterministic fractal models.

Constrained constructive optimization (CCO). Similar to fractal modeling (items 2 and 3 above) CCO also aims at representing the vascular tree by single segments rather than by compartments. However, the present method of CCO neither uses anatomical knowledge to arrange the segments geometrically nor does it resort on statistical properties of vessel segments. Hence, it is even more surprising that these can be reproduced fairly well by constrained constructive optimization alone. Its key mechanism draws on two concepts: (*a*) right from the start, the geometric arrangement of segments is considered important and at any stage influences the future growth of the tree. Hence, configurations which are geometrically meaningless cannot even occur and arrangeability in space remains guaranteed at any time. In fractal terminology we may say that the existing transient structure itself constitutes the major part of the generator which, as a consequence, concomitantly develops. (*b*) The stochastic process of adding terminals is not a priori defined (like in the case of stochastic fractal models) but is constantly and implicitely influenced via the structure already existing: tossing for terminal sites is repeated until the distance to an existing segment exceeds a (declining) threshold, so that new terminals are preferentially added within regions of hitherto low density (of terminals).

Finally, calculated statistical and hemodynamic properties, serving as criterions for the fidelity in modeling a real tree, emerge from CCO without any possibility to plug them in or alter them by intent. If the boundary conditions and the target function are selected properly, the resulting tree will yield realistic statistics and hemodynamic characteristics. And hence we may envisage to test several choices of (boundary conditions and target functions for) CCO against each other, so as to get more insight into the targets and rules that might have governed the evolutionary process of arterial trees in mammals.

The authors thank Mrs. R. Krenn, MS. and Mrs. B. Funk for preparing the figures. Thanks for valuable discussions are due to the other members of the Working Group for Biomedical Computersimulation, Dr. G. Laufer and Dr. A. Moritz.

This work was supported by the Ludwig Boltzmann Institut für Herzchirurgische Forschung and the Bundesministerium für Wissenschaft und Forschung, Grant 49.820/4-24/92.

Original version received 16 June 1993 and accepted version received 27 December 1993.

REFERENCES

Arts, T., R. T. I. Kruger, W. van Gerven, J. A. C. Lambregts, and R. S. Reneman. 1979. Propagation velocity and reflection of pressure waves in the canine coronary artery. *American Journal of Physiology.* 237:H469–H474.

Dawant, B., M. Levin, and A. S. Popel. 1985. Effect of dispersion of vessel diameters and lengths in stochastic networks I. Modeling of microcirculatory flow. *Microvascular Research.* 31:203–222.

Fung, Y. C. 1984. Biodynamics: Circulation. Springer-Verlag, New York. 82–85.

Kamiya, A., and T. Tatsuo. 1972. Optimal branching structure of the vascular tree. *Bulletin of Mathematical Biophysics.* 34:431–438.

Lefevre, J. 1983. Teleonomical optimization of a fractal model of the pulmonary arterial bed. *Journal of Theoretical Biology.* 102:225–248.

Levin, M., B. Dawant, and A. S. Popel. 1986. Effect of dispersion of vessel diameters and lengths in stochastic networks II. Modeling of microvascular hematocrit distribution. *Microvascular Research.* 31:223–234.

Milnor, W. R. 1989. Hemodynamics. Williams and Wilkins, Baltimore, MD. 32–35.

Pelosi, G., G. Saviozzi, M. G. Trivella, and A. L'Abbate. 1987. Small artery occlusion: a theoretical approach to the definition of coronary architecture and resistance by a branching tree model. *Microvascular Research.* 34:318–335.

Rodbard, S. 1975. Vascular Caliber. *Cardiology.* 60:4–49.

Rooz, E., T. F. Wiesner, and R. M. Nerem. 1985. Epicardial coronary blood flow including the presence of stenosis and aorto-coronary bypasses. I. Model and numerical method. *ASME Journal of Biomechanical Engineering.* 107:361–367.

Smaje, L. A., P. A. Fraser, and G. Clough. 1980. The distensibility of single capillaries and vessels in the cat mesentary. *Microvascular Research.* 20:358–370.

Thompson, D. W. 1952. On growth and form. Volume II. Cambridge University Press, Cambridge, UK. 948–957.

West, B. J., and A. L. Goldberger. 1987. Physiology in fractal dimensions. *American Scientist.* 75:354–364.

Zamir, M. 1978. Nonsymmetrical bifurcations in arterial branching. *Journal of General Physiology.* 72:837–845.

Zamir, M., and H. Chee. 1986. Branching characteristics of human coronary arteries. *Canadian Journal of Physiology and Pharmacology.* 64:661–668.

Zamir, M., and H. Chee. 1987. Segment analysis of human coronary arteries. *Blood Vessels.* 24:76–84.

Zamir, M. 1988. Distributing and delivering vessels of the human heart. *Journal of General Physiology.* 91:725–735.